

Random-field-induced spin-glass-like behavior in the diluted Ising antiferromagnet $\text{Fe}_{0.31}\text{Zn}_{0.69}\text{F}_2$

F. C. Montenegro,* A. R. King, and V. Jaccarino

Department of Physics, University of California, Santa Barbara, California 93106

S.-J. Han and D. P. Belanger

Department of Physics, University of California, Santa Cruz, California 95064

(Received 14 November 1990)

The evolution of the $d=3$ random-field Ising model (RFIM) in the strong-dilution limit has been studied using Faraday-rotation techniques on the Ising antiferromagnet $\text{Fe}_{0.31}\text{Zn}_{0.69}\text{F}_2$. Particular attention has been given to the external field (H) dependence of the phase transition $T_c(H)$ and the equilibrium boundary $T_{\text{eq}}(H)$ in the range $0 \leq H \leq 7$ T. For $H < 1$ T, both $T_N - T_c(H)$ and $T_N - T_{\text{eq}}(H)$ scale as $H^{2/\phi}$, with $\phi=1.42$, the universal $d=3$ random-exchange-to-RFIM crossover exponent. However, as the field is increased above $H=1.5$ T, a striking reversal of the curvature of $T_{\text{eq}}(H)$ versus T is observed, now scaling with H as does the de Almeida-Thouless replica symmetry-breaking line in a conventional, exchange-frustrated spin glass, $T_N - T_{\text{eq}}(H) \approx H^{2/\phi}$, with $\phi=3.4$. Other spin-glass-like behavior is seen at higher fields such as the time dependence of the hysteretic properties of the remanent magnetization. These observations suggest it is the large random field that induces spin-glass-like behavior in this diluted antiferromagnet, without significant (if any) exchange frustration being present.

INTRODUCTION

The randomly (site) diluted uniaxial antiferromagnet (AF) has been the proverbial testing ground for specific models of Ising random magnetism. Of all those studied, $\text{Fe}_x\text{Zn}_{1-x}\text{F}_2$ has become the prototypical system for delineating the static and dynamic critical behavior of the random-exchange (REIM) and random-field Ising model (RFIM) universality classes, in external fields $H=0$ and $H>0$, respectively.^{1,2}

It has been tacitly assumed in the earlier experimental and theoretical studies of the RFIM problem that the identification of the diluted AF, in a uniform H , with the ferromagnet in a site-random field was only to be made for small H/J and weak dilution.³ The latter condition presumes one stays well away from the site percolation concentration⁴ x_p which, for the $\text{Fe}_x\text{Zn}_{1-x}\text{F}_2$ system, is $x_p=0.24$ for the dominant exchange interaction. (In FeF_2 the overwhelmingly dominant exchange interaction J_2 is the AF one between any given spin and its eight nearest neighbors on the opposite sublattice.⁵) This can be seen most clearly insofar as the usual Imry-Ma statistical arguments,⁶ which lead to a lower critical dimension $d_l=2$, become inapplicable as x approaches x_p . All of the definitive studies of the critical behavior of the REIM and RFIM universality classes and the hysteretic phenomena associated with the extreme critical slowing down in the $d=3$ RFIM system have, in fact, been made for $x \geq 0.46$.^{1,2}

Nevertheless, there has been theoretical interest in the nature of the phase diagram of the diluted AF for all ranges of H/J and strong randomness, i.e., $x \ll 1$. It has been argued by Föhnle⁷ that the long-range order will become unstable for small H as x approaches x_p from

above. Bray⁸ has suggested that relaxation times will become extremely long for $T \approx T_N(1)/z$, where $T_N(1)$ is the transition temperature at $x=1$ and z is the number of exchange-coupled neighbors ($T_N=78.4$ K and $z=8$ for FeF_2). Under certain mean-field approximations and with no exchange frustration included, a glassy phase has been predicted by de Almeida and Bruinsma⁹ for small x and large H/J . Replica symmetry breaking is obtained along a de Almeida-Thouless line, as would be the case in a canonical, exchange-frustrated spin glass. Moreover, recent experiments¹⁰⁻¹³ on $\text{Fe}_x\text{Zn}_{1-x}\text{F}_2$ at, or just slightly above x_p do exhibit many of the properties of more conventional (exchange-frustrated) spin-glass systems. Indeed, if this is the case, one is led to ask just how the system evolves from REIM-RFIM behavior at large x to spin-glass-like behavior at smaller x , as a function of x and H .

In this work, we investigate the critical behavior and nonequilibrium properties of the $\text{Fe}_{0.31}\text{Zn}_{0.69}\text{F}_2$ system in a uniform field, $\mathbf{H} \parallel \mathbf{c}$ axis, using the Faraday-rotation technique. The Fe concentration $x=0.31$ is large enough so that one would still expect to find a long-range-ordered AF state at $H=0$. A comparison neutron-scattering study¹⁴ of the same crystal provides additional insight into the nature of the ordering in the H - T plane. Previous vibrating sample magnetometer measurements^{12,13} on the $x=0.31$ system established an unusual shape to the equilibrium boundary, $T_{\text{eq}}(H)$. In particular, a reversal in the curvature of $T_{\text{eq}}(H)$ versus H was observed at $H \approx 2$ T, which had not been found at either smaller ($x=0.24$) or larger ($x=0.46$) concentrations. The present study further elucidates the nature of $T_{\text{eq}}(H)$, and establishes the behavior of the phase transition $T_c(H)$ in this system.

EXPERIMENTAL METHOD

Faraday-rotation (FR) studies were performed on a single-crystal of $\text{Fe}_{0.31}\text{Zn}_{0.69}\text{F}_2$. The polished crystal has dimensions $6.7 \times 6.7 \times 3.3 \text{ mm}^3$ with the c axis perpendicular to one set of $6.7 \times 3.3 \text{ mm}^2$ faces. The concentration was determined using calibrated density measurements and its concentration gradient was determined by using the scanning optical birefringence technique.¹⁵ Along the growth axis, which is perpendicular to the direction of the c axis in this crystal, the measured total variation in x is $\delta x = 0.0045$. The concentration gradients perpendicular to the growth axis are much smaller. Since the laser beam is directed along the c axis, it is perpendicular to the gradient direction. Hence, the effect of the gradient along the growth axis is minimized. Although the neutron-scattering measurements on the same crystal, which sampled the full gradient, showed an apparent rounding^{14,16} of the transition of about 0.7 K, we believe the transition rounding in the FR experiments to be at least an order of magnitude smaller and hence inconsequential to the following analysis and discussion.

Measurements were made using two different systems. The initial low-field measurements ($H \leq 1.5 \text{ T}$) utilized an iron core magnet, while the high-field measurements ($H \leq 7 \text{ T}$) were made using a split coil superconducting magnet. The low-field technique utilized no mirrors, since the magnet has optical access through the pole faces. The split coil arrangement of the superconducting magnet, on the other hand, required the use of one front surface mirror to direct the laser beam along the crystal c axis.

The arrangement of optical components in the small H apparatus is straightforward and is similar to that previously described.¹⁷ The laser beam, polarized by the first polarizer, goes in turn through the sample, photoelastic modulator, and second polarizer before reaching the detector. The last polarizer is fixed at an angle $\pi/4$ relative to the axes of the modulator for maximum sensitivity. The first polarizer is rotated to follow the Faraday rotation. One can also obtain equivalent results with an arrangement of the optical components in which the positions of the laser and detector are switched.

The large- H arrangement is different since the reflection at the front surface mirror has to be taken into consideration. A schematic representation of the optical configuration is shown in Fig. 1. A He-Ne laser beam ($\lambda = 632.8 \text{ nm}$) is polarized perpendicular (or parallel) to the plane of incidence of the mirror via the first polarizer. Only in this way will the mirror reflection not introduce an unwanted elliptical component into the beam. The beam is directed by the mirror through the sample in a direction parallel to both the c axis and the applied field. The optical axes of the photoelastic modulator (**M**), which operates at a frequency $\omega = 50 \text{ kHz}$, are fixed at an angle $\pi/4$ relative to the axes of the analyzing polarizer (**A**). **M** and **A** rotate together as a unit. We use phase-sensitive detection with a computer control feedback system to determine the 2ω null point in the optical signal.¹⁷ The resolution of the rotation is better than 0.005° with a typical noise level.

The crystal was mounted on a copper sample holder attached to a cold finger. The temperature was measured and stabilized using a carbon thermometer. Typically, the temperature stability was better than 1 mK over the range $5 < T < 40 \text{ K}$ and the absolute accuracy was about 0.1 K.

Significant hysteresis is observed at low temperatures. Hence, we employed two procedures for measurements. In the first zero-field cooling (ZFC), we cool the crystal in zero field to a given temperature, then raise the field, and finally raise the temperature. We obtain data upon increasing T , stabilizing the temperature before each reading. In the second procedure field-cooling (FC) data are obtained upon cooling in the field, with the temperature stabilized before each reading.

EXPERIMENTAL RESULTS

We first consider the results obtained at relatively low fields; $H \leq 1.5 \text{ T}$. In Fig. 2 we show the measured FR angle Θ , which is proportional¹⁷ to the uniform magnetization as a function of temperature T for three fields,

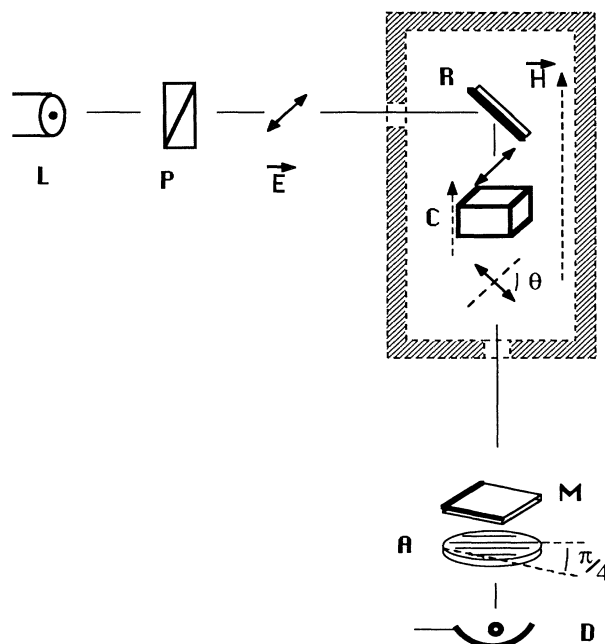


FIG. 1. Schematic representation of the optical arrangement used in the high-field measurements. A light beam from a He-Ne laser (**L**) is polarized with a calcite polarizer (**P**). A front surface mirror (**R**) is necessary to direct the beam along the field direction and the electric field (E) is perpendicular to the plane of incidence. E is rotated by an angle Θ as it passes through the crystal which is oriented with its c axis along H . The double-walled box indicates the cryostat which has a split coil superconducting magnet for measurements with $H \leq 7 \text{ T}$. The photoelastic modulator (**M**) and analyzing polarizer (**A**) are rotated together with their optical axes fixed at an angle of 45° with respect to each other until the proper null signal reaches the detector (**D**).

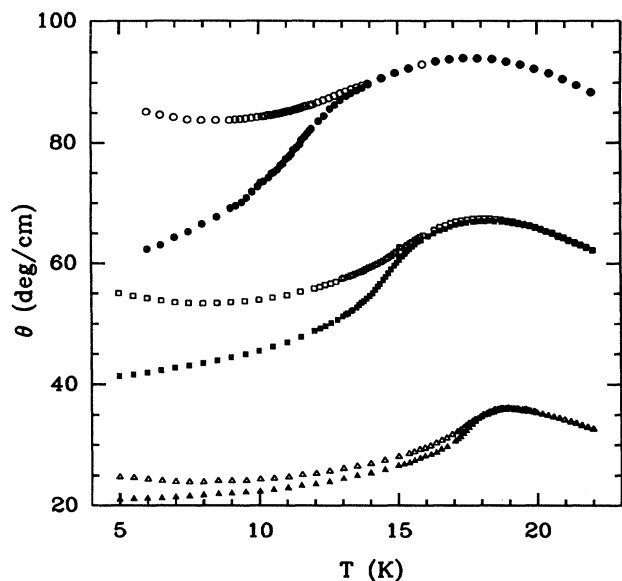


FIG. 2. Θ vs T for $H=0.5, 1.0,$ and 1.5 T. The solid symbols represent data taken upon ZFC and the open symbols are for FC. $T_c(H)$ is at the inflection point in Θ versus T of the ZFC data. $T_{eq}(H)$ is the point at which the ZFC and FC data no longer coincide.

$H=0.5, 1.0,$ and 1.5 T, following both zero-field-cooling (ZFC) and field-cooling (FC) procedures. A dramatic hysteresis is seen in the FC and ZFC results below a temperature $T_{eq}(H)$, defined as the temperature above which all measurements give results independent of the field-cycling procedure. Note that the difference between the ZFC and FC results becomes more pronounced as the field increases. In the critical region, the temperature derivative $d\Theta/dT$ vs T has been demonstrated to be proportional to the magnetic specific heat C_m in dilute antiferromagnets.¹⁷⁻¹⁹ $d\Theta/dT$ vs T is shown in Fig. 3 for $H=0.05, 0.5,$ and 1.0 T. Just as with higher concentrations^{1,2} $x \geq 0.46$, C_m exhibits a symmetric peak rounded by the extreme critical slowing down that occurs near the phase transition $T_c(H)$. The observation of a symmetric, dynamically rounded divergence, particularly in the ZFC measurements, is indicative of the existence of $d=3$ RFIM critical behavior in the $\text{Fe}_x\text{Zn}_{1-x}\text{F}_2$ systems^{1,2} $T_c(H)$ and $T_{eq}(H)$ can be accurately determined from the $d\Theta/dT$ versus T data since neither the peak position nor the point at which hysteresis is observed is strongly dependent upon the measurement time as long as $H \leq 1.5$ T. That antiferromagnetic long-range ordering (AF LRO) is associated with the ZFC peak has been verified in neutron-scattering experiments¹⁴ on the same crystal.

Quite different behavior is observed at larger fields. Figure 4 shows Θ vs T for $H=3$ T for both the ZFC and FC procedures. Although appearing qualitatively similar to the low-field scans shown in Fig. 2, there is, in fact, a crucial difference. While there is an inflection point in Θ versus T for the ZFC data, the position and shape of the curve are strongly dependent on the scanning rate.

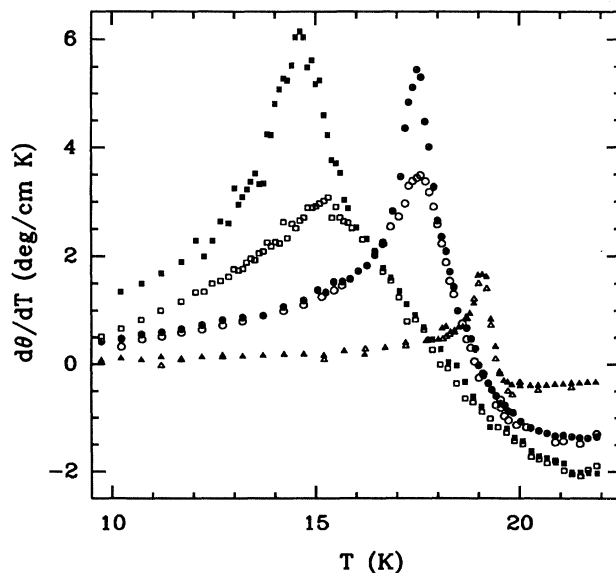


FIG. 3. $d\Theta/dT$ vs T for $H=0.05$ T, 0.5 T, and 1.0 T. The solid symbols represent data taken upon ZFC and the open symbols are for FC. The ZFC peaks are proportional to the specific heat and are dynamically rounded. The FC peaks are suppressed since the long-range-order AF ground state is not achieved via this procedure.

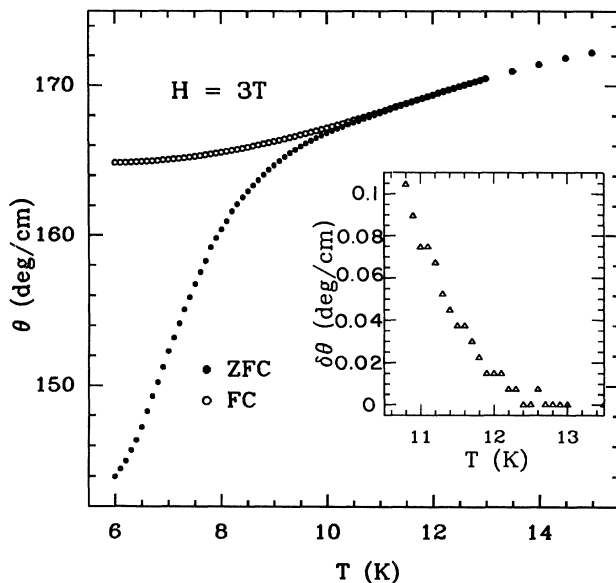


FIG. 4. Θ vs T for $\text{Fe}_{0.31}\text{Zn}_{0.69}\text{F}_2$ for $H=3$ T. Although qualitatively resembling the low- H data, the inflection point in the Θ vs T ZFC data with $H=3$ T now exhibits a very strong dependence on the time taken to measure each data point, unlike the data below $H=1.5$ T. This shows that, unlike measurements at low H , the point of inflection is a consequence of a dynamical effect and does not necessarily imply a phase transition exists. The insert shows the difference, $\delta\Theta$, between the FC and ZFC angle vs T . $T_{eq}(H)$ is the point above which $\delta\Theta=0$.

Hence, this feature cannot readily be identified with a phase boundary [i.e., $T_c(H)$], as is the case for small fields. Indeed, the neutron-scattering measurements¹⁴ do show that the low- T region for $H > 2$ T is *not* associated with AF LRO. The value of $T_{eq}(H)$ obtained, on the other hand, is not significantly rate dependent for the range of rates used in these measurements and could therefore be consistently determined.

All of the data for $T_c(H)$ and $T_{eq}(H)$ for $0 < H < 7$ T are shown in Fig. 5. We demonstrate below that the lower-field portion of the diagram corresponds to the RFIM behavior observed previously for $x \geq 0.46$. However, the large- H behavior has not been observed at any field for $x \geq 0.46$.

The time dependence of the magnetization was investigated for the H - T region above the extrapolation of $T_c(H)$ and below $T_{eq}(H)$. First, the crystal was ZFC to $T=6.5$ K. Then the field was increased rapidly to $H=4$ T and the Faraday rotation was recorded as a function of time. A monotonic increase in the uniform magnetization with time indicates that more spins are becoming aligned with the applied field as time increases. This corresponds to the observation in the neutron-scattering experiments¹⁴ that, under similar conditions, the *staggered* magnetization decreases as H increases.

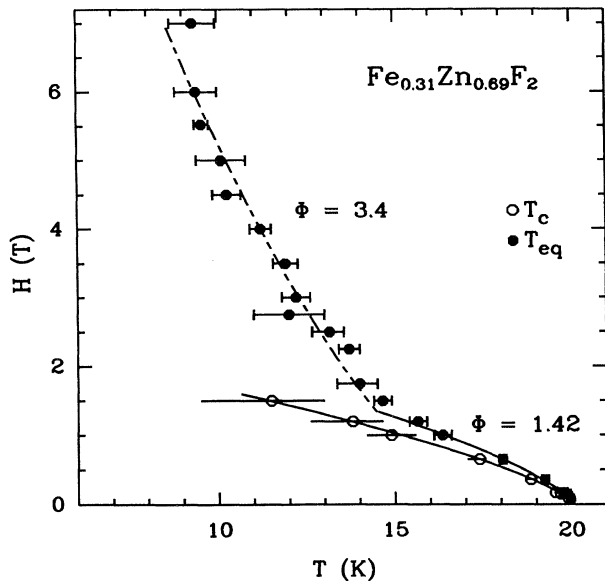


FIG. 5. The T vs H phase diagram of the $\text{Fe}_{0.31}\text{Zn}_{0.69}\text{F}_2$ RFIM system. Error bars are given for the $T_{eq}(H)$ measurements. The horizontal bars through the ZFC $T_c(H)$ data represent the dynamical rounding of the transition as indicated by the inflection points in $d\Theta/dT$ vs T . The solid and dashed curves represent the scaling behavior for low and high field with $\phi=1.42$ and 3.4 , respectively. For large H , following ZFC, inflection points in Θ versus T could be observed, but were very time dependent in shape and location. Hence, they are not identified with $T_c(H)$, as was the case for low H .

INTERPRETATION

The field dependence of $T_c(H)$ and $T_{eq}(H)$ in the low-field region is shown in Fig. 6. The data precisely follow the REIM to RFIM crossover scaling behavior as indicated by the solid curves, representing $T_N - T_c(H) \approx H^{2/\phi}$ and $T_N - T_{eq}(H) \approx H^{2/\phi}$, respectively, with $\phi=1.42$. (The mean-field correction, $-bH^2$, is entirely negligible compared to the RF shift at small x .^{1,2}) This value for the crossover exponent ϕ has been determined from previous experiments at several larger magnetic concentrations.^{1,2} For comparison purposes, we show in Fig. 7 results that were earlier obtained for $x=0.46$. Hence, we see at low H there is a universal REIM to the RFIM crossover scaling behavior in $T_c(H)$ and $T_{eq}(H)$. This is in keeping with the neutron-scattering measurements which show AF LRO below $H=1$ T and $T < T_c(H)$ and the critical behavior at small H to be consistent with what is observed at higher concentrations.^{1,2} Thus, in all respects, the small- H behavior in $\text{Fe}_{0.31}\text{Zn}_{0.69}\text{F}_2$ is analogous to that seen for $x \geq 0.46$.

Only when $H > 1.5$ T is there any feature found which distinguishes the behavior in $\text{Fe}_{0.31}\text{Zn}_{0.69}\text{F}_2$ from that observed at any measured field for $x \geq 0.46$. Beginning at about $H=1.5$ T a reversal in the curvature of $T_{eq}(H)$ versus H occurs, consistent with previous observations.^{12,13} Figure 5 shows the large-field behavior and a fit to the scaling behavior $T_N - T_{eq}(H) \approx H^{2/\phi}$, with the fixed value $\phi=3.4$, indicated by the dashed curve. This is to be contrasted with the small- H scaling where $\phi=1.42$, as indicated by the solid curves in Fig. 5. The particular choice of $\phi=3.4$ for the large- H scaling in Fig. 5 is motivated by the observation of a similar scaling to the

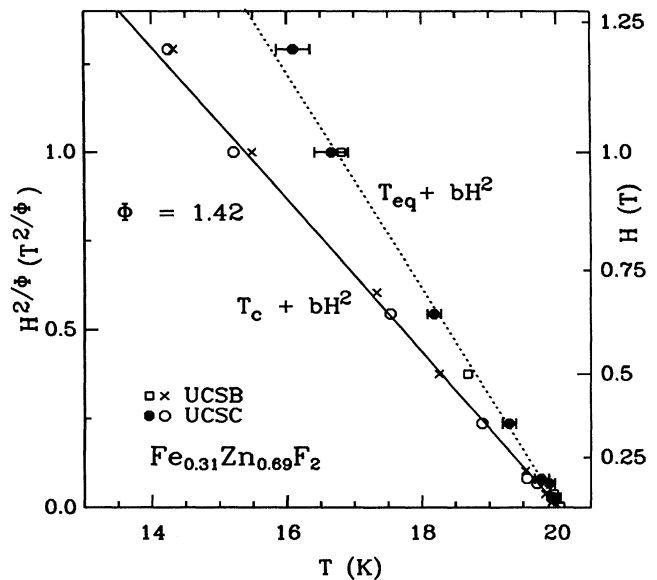


FIG. 6. $T_c(H)$ and $T_{eq}(H)$ vs T , with the appropriate mean-field correction, for the $\text{Fe}_{0.31}\text{Zn}_{0.69}\text{F}_2$ system at low H . The straight lines represent fits to $H^{2/\phi}$ with $\phi=1.42$, the REIM to RFIM crossover exponent.

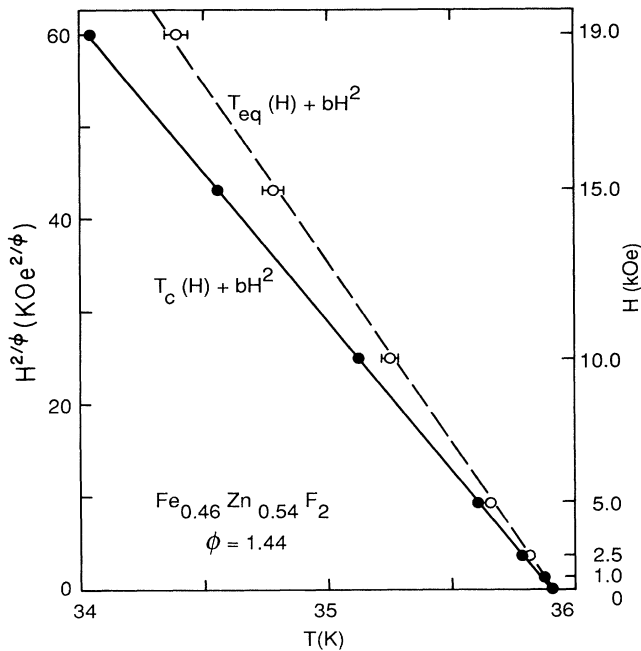


FIG. 7. $T_c(H)$ and $T_{eq}(H)$ vs T , with the appropriate mean-field correction, for the $\text{Fe}_{0.46}\text{Zn}_{0.54}\text{F}_2$ system. The straight lines represent fits to $H^{2/\phi}$ with $\phi=1.44$, the REIM to RFIM crossover exponent. Note that, as a consequence of the smaller random-field strength in this system relative to the $x=0.31$ one, the shifts in $T_c(H)$ and $T_{eq}(H)$ are much smaller than those shown in Fig. 6. Data taken from Ref. 24.

equilibrium boundary^{10–13} in $\text{Fe}_{0.25}\text{Zn}_{0.75}\text{F}_2$ (see Fig. 8 taken from Ref. 10), whose Fe concentration is essentially at the percolation threshold, $x_p=0.24$. In the $x=0.25$ case, the $T_{eq}(H)$ boundary, with $\phi=3.4$, extends from $H=0$ to the largest H measured, $H=7$ T. Neutron-scattering results show no AF LRO exists at $x \approx x_p$, even for $H=0$.²⁰ Likewise, neutron-scattering measurements¹⁴ in $\text{Fe}_{0.31}\text{Zn}_{0.69}\text{F}_2$ have shown the upper part of the $T_{eq}(H)$ boundary is not associated with the onset of AF LRO, as it is in the small- H region. This suggests that no AF LRO exists below $T_{eq}(H)$ when the field scaling exponent $\phi \approx 3.4$ at any x in the range $0.24 \leq x \leq 0.31$.

The scaling behavior $T_N - T_{eq}(H) \approx H^{2/\phi}$, with $\phi=3.4$, is similar to that observed in conventional spin-glass systems. The boundary is associated with the de Almeida–Thouless (AT) replica symmetry-breaking line.²¹ The AT-like boundary in $\text{Fe}_{0.31}\text{Zn}_{0.69}\text{F}_2$ at large fields and the fact that the boundary is not associated with the onset of AF LRO would appear to suggest a spin-glass state occurs at large H for $T < T_{eq}(H)$. However, the conventional models of spin glasses have as necessary ingredients two features; randomness in the exchange and frustration. Hence, the conventional spin-glass model does not correspond to the $\text{Fe}_{0.31}\text{Zn}_{0.69}\text{F}_2$ system since there is little, if any, exchange frustration.⁵ This is evident in the AF LRO ground state at $H=0$. Instead, the spin-glass-like behavior must be a manifesta-

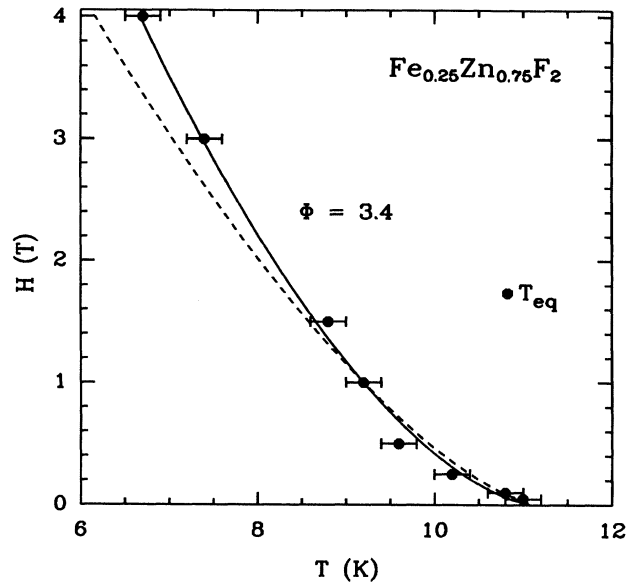


FIG. 8. $T_{eq}(H)$ vs T for $\text{Fe}_{0.25}\text{Zn}_{0.75}\text{F}_2$, obtained from magnetization measurements. The solid curve is a fit to $T_c(H) \approx H^{2/\phi}$ with $\phi=3.4$, and the dotted curve is a fit with the de Almeida–Thouless exponent $\phi=3$. Data taken from Ref. [10].

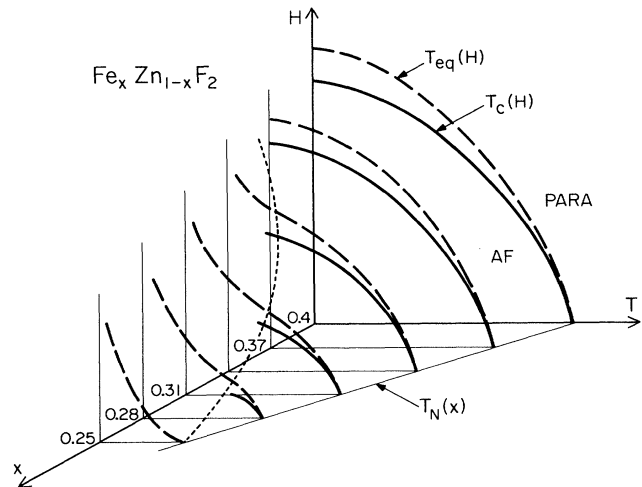


FIG. 9. The schematic evolution of the H vs T phase diagram for the $\text{Fe}_x\text{Zn}_{1-x}\text{F}_2$ system with x . As x decreases, the high-field behavior occurs in $T_{eq}(H)$ probably first above $x \approx 0.37$. As x approaches $x_p=0.24$, the spin-glass-like portion of the phase diagram increases and the antiferromagnetic portion shrinks. At $x=0.24$, the antiferromagnetic part has vanished and the only feature remaining is $T_{eq}(H)$, with a de Almeida–Thouless-like curvature, and there is no AF LRO. The small dashed curve represents the x dependence of the crossover from the low- to high- H regions.

tion of the breakdown of the small- H limit of the RFIM in dilute antiferromagnets. The field at which this occurs must approach zero as x approaches x_p , since it occurs for all H in $\text{Fe}_{0.25}\text{Zn}_{0.75}\text{F}_2$. Hence, the spin-glass-like behavior observed at $H=0$ in the latter system is most likely a result of an instability to vanishingly small random fields.

From the observations in $\text{Fe}_x\text{Zn}_{1-x}\text{F}_2$ at concentrations $x \geq 0.46$, $x=0.31$, and $x=0.25$, a schematic evolution of the $T_{\text{eq}}(H)$ boundary as x approaches x_p has been proposed²² and is depicted in Fig. 9. The large- x regime is entirely described by scaling with $\phi=1.42$. Somewhere above $x \approx 0.37$, in addition to the low-field behavior with $\phi=1.42$, the high-field behavior, with $\phi=3.4$, would first appear. The low-field region, corresponding closely to the onset of AF LRO, shrinks rapidly as x approaches x_p and the large- H scaling becomes the sole feature of $T_{\text{eq}}(H)$. There is as yet no firm theoretical understanding of this novel feature associated with the evolution of the phase diagram versus x .

To summarize, we have extensively characterized the phase diagram of a RFIM system just above the magnetic percolation threshold. The nature of a previously observed^{12,13} novel feature of the phase diagram of the RFIM at large fields has been further elucidated. $T_{\text{eq}}(H)$ has reversed curvature relative to the small- H behavior, the latter being the universal REIM to RFIM crossover behavior observed previously for $x \geq 0.46$. In the small- H region, $T_c(H)$ scales in the universal way, $T_N - T_c(H) \approx H^{2/\phi}$ with $\phi=1.42$ at low H and T , and

forms the boundary of the AF LRO region. $T_{\text{eq}}(H)$ lies just above $T_c(H)$ for $H < 1.5$ T. In the large- H region, $H > 1.5$ T, the behavior is similar to that seen at all H for $\text{Fe}_{0.25}\text{Zn}_{0.75}\text{F}_2$. $T_{\text{eq}}(H)$ scales as $T_N - T_c(H) \approx H^{2/\phi}$ with $\phi=3.4$ as does the de Almeida–Thouless replica symmetry-breaking line in spin glasses, and departs widely from the extrapolation of $T_c(H)$; the large region between them exhibits very slow dynamics and no AF LRO. Therefore, at larger fields $T_{\text{eq}}(H)$ is not associated with the immediate onset of AF LRO. We have suggested the likely evolution of the $T_{\text{eq}}(H)$ boundary as x approaches the percolation threshold. Further investigations, with $0.2 < x < 0.4$, are needed to determine how the large- H behavior first manifests itself as x is decreased and how it finally becomes the sole feature of the phase diagram as the AF region disappears. Although instabilities have been suggested in theories of the dilute antiferromagnet in an applied field as x approaches x_p , a clearer understanding²³ needs to be developed in light of the new results.

ACKNOWLEDGMENTS

This work was supported at the University of California at Santa Cruz by Department of Energy No. DE-FG03-87ER-45324 and at the University of California at Santa Barbara by NSF Grant No. NSF-DMR88-15560. One of the authors (F.C.M.) was partially supported by CNPq (Brazilian agency).

*Permanent Address: Departamento de Física, Universidade Federal de Pernambuco, 50739, Recife, PE, Brasil.

¹V. Jaccarino and A. R. King, *Physica A* **163**, 291 (1990).

²D. P. Belanger, *Phase Trans.* **11**, 53 (1988).

³S. Fishman and A. Aharony, *J. Phys. C* **12**, L729 (1979).

⁴M. F. Sykes and J. W. Essam, *Phys. Rev.* **133**, A310 (1964).

⁵M. T. Hutchings, B. D. Rainford, and H. J. Guggenheim, *J. Phys. C* **3**, 307 (1970).

⁶Y. Imry and S.-k. Ma, *Phys. Rev. Lett.* **35**, 1399 (1975).

⁷M. Fahnle, *Phys. Rev. B* **27**, 5821 (1983).

⁸A. J. Bray, *J. Phys. C* **16**, 5875 (1983).

⁹J. R. L. de Almeida and R. Bruinsma, *Phys. Rev. B* **37**, 7267 (1987).

¹⁰F. C. Montenegro, M. D. Coutinho-Filho, and S. M. Rezende, *Europhys. Lett.* **8**, 383 (1989).

¹¹S. M. Rezende, F. C. Montenegro, M. D. Coutinho-Filho, C. C. Becerra, and A. Paduan-Filho, *J. Phys. (Paris) Colloq.* **49**, C8-1267 (1988).

¹²F. C. Montenegro, U. A. Leitao, M. D. Coutinho-Filho, and S. M. Rezende, *J. Appl. Phys.* **67**, 5243 (1990).

¹³S. M. Rezende, F. C. Montenegro, U. A. Leitao, and M. D. Coutinho-Filho, in *New Trends in Magnetism*, edited by M. D. Coutinho-Filho and S. M. Rezende (World Scientific, Singapore, 1989), p. 44.

¹⁴D. P. Belanger, Wm. Murray, Jr., F. C. Montenegro, A. R. King, V. Jaccarino and R. W. Erwin, following paper, *Phys.*

Rev. B **44**, 2161 (1991).

¹⁵A. R. King, I. B. Ferreira, V. Jaccarino, and D. P. Belanger, *Phys. Rev. B* **37**, 219 (1988).

¹⁶D. P. Belanger, A. R. King, I. B. Ferreira, and V. Jaccarino, *Phys. Rev. B* **37**, 226 (1988).

¹⁷W. Kleemann, A. R. King, and V. Jaccarino, *Phys. Rev. B* **34**, 479 (1986).

¹⁸K. E. Dow and D. P. Belanger, *Phys. Rev. B* **39**, 4418 (1989).

¹⁹U. A. Leitao and W. Kleemann, *Phys. Rev. B* **35**, 8696 (1987).

²⁰D. P. Belanger and H. Yoshizawa (unpublished).

²¹J. R. L. de Almeida and D. J. Thouless, *J. Phys. A* **11**, 983 (1978).

²²V. Jaccarino and A. R. King, in *New Trends in Magnetism*, edited by M. D. Coutinho-Filho and S. M. Rezende (World Scientific, Singapore, 1990), p. 70.

²³One might ask whether dipolar interactions in dilute AF result in long-range forces which significantly alter the observed behavior. It has been shown that when FC metastable domains have been formed, dipolar interactions inhibit equilibration [T. Nattermann, *J. Phys. A* **21**, L645 (1988)]. In the equilibrium state, on the other hand, dipolar interactions do not yield long-range forces [H. S. Toh and G. A. Gehring, *J. Phys. A* (to be published)].

²⁴A. R. King, V. Jaccarino, D. P. Belanger, and S. M. Rezende, *Phys. Rev. B* **32**, 503 (1985).